

ANTENNA DESIGN TRADEOFFS FOR DENSE DISTRIBUTED RADAR NETWORK FOR WEATHER SENSING

Jorge L. Salazar, Eric A. Knapp, and David J. McLaughlin

Engineering Research Center for Collaborative Adaptive of the Atmosphere (CASA)
Dept. of Electrical and Computer Engineering, University of Massachusetts, USA
(jlsalaza@engin.umass.edu, knapp@ecs.umass.edu, and mclaughlin@ecs.umass.edu)

Abstract-This paper discusses trade-offs in key design parameters for networks of low-power electronically scanned phased array antennas. Such systems are currently being investigated for use in future weather networks capable of making observations in the lower troposphere and particularly the boundary layer. We consider how azimuth resolution, minimum radar sensitivity and polarimetric figures-of-merit vary for three different configurations of a dense radar network design and develop order-of-magnitude estimates for the cost and technological complexity associated with these panels.

I. INTRODUCTION

Today's long range (100-200 km or more) weather radar networks [1] do a very capable job sampling the middle and upper-parts of the troposphere and supporting hazardous weather warning and weather-related decision-support needs in multiple sectors of the economy. A fundamental property associated with any long range radar, however, is its inability to observe the lower troposphere and in particular the atmospheric boundary layer over much of its coverage range, owing to the blockage associated with the curvature of the earth. The WSR-88D network of Doppler radars in the US, for example, is capable of observing essentially the entire tropospheric volume at heights greater than 3 km above the surface of the earth. In contrast, this system observes $\sim 66\%$ of the volume at a height of 2 km, and only $\sim 33\%$ of the volume at 1 km height.

A new weather radar design concept currently being investigated by the NSF Center for Collaborative Adaptive Sensing of the Atmosphere (CASA) involves the use of dense networks of X-band radars that defeat the blockage effect of earth's curvature by limiting the operating range of each radar to a few tens of km. Such networks would be arranged in deployments comprised of tens (urban environment), hundreds (regional deployment), or potentially even thousands of radar nodes (covering a nation the size of the contiguous US, for example) for comprehensive sampling of lower troposphere and boundary layer. A key barrier to realizing such a technology is the present unavailability of physically-small, low-cost

measurement-quality radars that would be practically and cost-effectively deployed in such networks. This paper addresses several aspects of the design of small electronically scannable solid state radars that are being pursued in the CASA center. We consider the design of radar "panels" that would deploy on existing cellular communication or other towers as illustrated in Figure 1. To provide for 360 degrees of azimuth coverage

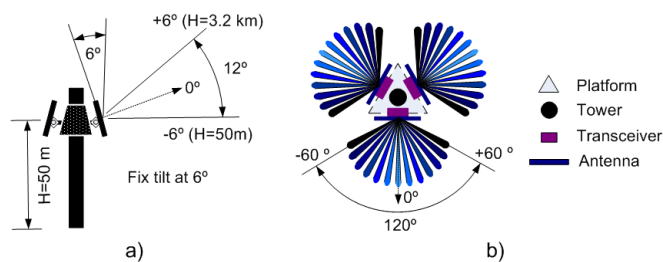


Fig. 1. a) Setup for electronic scan of 12 degrees (± 6) degrees in elevation at a 6 degree fixed tilt is used to achieve 100% coverage at 3 km of altitude b) Setup for electronic scan in azimuth plane using three sectors of 120 deg (± 60 deg).

using flat panels, at least three sectors have to be considered since it is not practical to scan beyond 90 deg from the broadside direction using such antenna arrays. We consider a design capable of electronically scanning up to a height of 3 km at maximum range of 30 km. When installed with a tilt of 6 degrees in elevation, such an antenna perform surveillance from ground-level to 3 km by electronically scanning over a range of 12 degrees (± 6 degrees from the antenna broadside or boresight direction). The problem of determining the optimum number of sectors for a multi-face planar array has been considered by Trunk [3] for the case when a single radar is considered for the target tracking and surveillance problem. In such a case, either three or four planar sectors proves to be the optimum design, depending on the specifics of the electrical properties of the antennas and the costs of the various components of the system. In this paper we address the design tradeoffs and seek to define the optimum system parameters (eg, network topology, sector and antenna configuration) for a dense network of such arrays for weather surveillance. The particular behavior being investigated here is the degradation in the performance of a phased array antenna as it scans away from the boresight

⁰This work was primarily supported by the Engineering Research Centers Program of the National Science Foundation under NSF Award Number 0313747. Any opinions, findings and conclusions or recommendations expressed in this material are those of the authors and do not necessarily reflect those of the National Science Foundation.

direction, and the effects of scan loss, beamwidth broadening, and cross-polarization contamination increasingly impact the measurement performance.

We evaluate the performance of resolution cell area, minimum measurement sensitivity, and polarization performance parameters in various scenarios in which planar phased arrays are deployed in different configurations of a dense radar network. Three different topological and antenna-sector deployment configurations are considered, as shown in Figure 2. Configuration A considers the case in which 3 panels (or sectors) each observing a 120 deg wide sector (± 60 deg), are deployed in a triangular lattice, or spatial repeat-pattern. Configuration B represents the case in which 4 sectors, each observing a 90 deg wide sector (± 45 deg) are deployed in a square spatial repeat-pattern. Configuration C represents the case in which 6 sectors, each observing a 60 deg sector (± 30 deg) are deployed in a triangular lattice. In each case, we consider a -25 dB peak sidelobe level and a physical aperture area of 1 m by 1 m. Such an antenna would achieve a 1.8 degree pencil beam radiating pattern in the broadside direction which serves as a baseline for performance comparison.

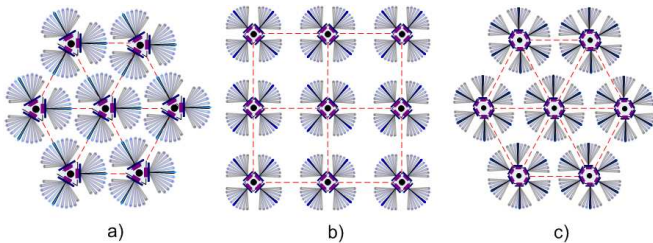


Fig. 2. a) Triangular grid with nodes of 3 sectors of 120 deg (± 60 deg), b) Square grid with nodes of four sectors of 90 deg (± 45 deg), and c) Triangular grid with nodes of 6 sectors of 60 deg (± 30 deg).

This paper is organized in 4 sections. Section 2 presents the performance used in this analysis and presents the behavior associated with a single radar node. Then, Section 3 expands the analysis and considers the performance for the dense network case. Section 4 establishes a very preliminary set of cost-performance considerations of the low-cost radars considered in this study

II. PERFORMANCE MODEL FOR SINGLE RADAR

A. Azimuth resolution performance model (A_{zr})

The radar azimuth resolution in terms of radar range and beamwidth of the antenna is expressed in the following equation.

$$A_{zr}(R, \phi) = R \sin(\phi) \quad (1)$$

where ϕ represent the 3 dB, or half-power, antenna beamwidth in the horizontal plane, and R represents the radar range in kilometers. For electronically scanned planar array antennas the beamwidth of the radiation pattern is not constant in angular space; it increases when the antenna beam is steered away from the broadside direction. The 3dB beamwidth is $\theta_3 = \theta_3(\text{broadside})B_b/\cos(\theta)$ as defined in the reference [4]

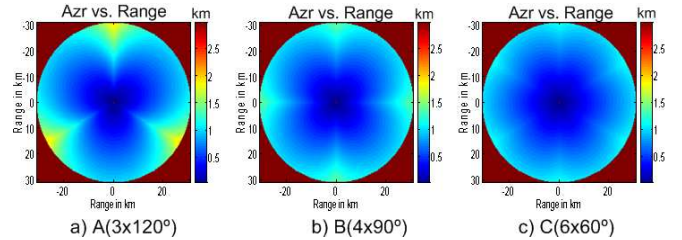


Fig. 3. A_{zr} (worst): a) 2.0 km, b) 1.4 km, and c) 1.1 km A_{zr} (median): a) 0.84 km, b) 0.8 km and c) 0.74 km. R_{max} :31 km, θ_o : -6 deg and H:50 m

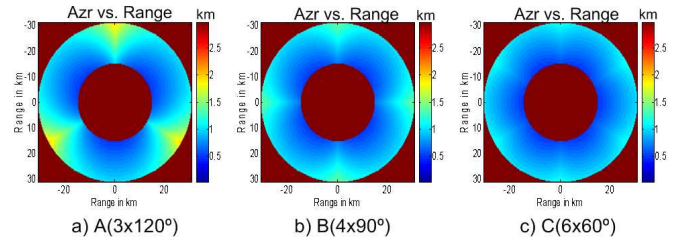


Fig. 4. A_{zr} (worst): a) 2.0 km, b) 1.42 km, and c) 1.2 km A_{zr} (median): a) 0.94 km, b) 0.88 km and c) 0.83 km. R_{max} :31 km and θ_o : +6 deg and H:3.18 Km

where B_b represents the beam broadening factor, having a reasonable value of 1.2 (corresponding to a -25 dB Taylor amplitude distribution.) The azimuthal resolution of a single radar having 3, 4, and 6 panels each with 1.8 degree broadside beamwidth and operated out to 30 km maximum range is shown Figure 3 and Figure 4. These three configurations represent single-radar instances of the multi-radar clusters for cases A, B, and C of Figure 2.

For each case considered, the planar arrays have 42 radiating antenna elements in the elevation plane. This number of elements is set by antenna design theory to avoid grating lobes when the antenna beam is steered to its maximum off-boresite direction of 6 deg. In the azimuth plane the number of radiating elements is 64, 60 and 54 for the configuration A (120 degree-wide sector, 60 deg from broadside), B (90 degree-wide, 45 deg from broadside) and configuration C (60 degree-wide, 30 deg from broadside). The product of the number of radiating elements in the elevation and azimuth planes is important in establishing the complexity and cost of the antenna design, as we discuss in Section IV

Figure 3 and Figure 4 show the azimuth resolution for these radars in configurations A, B, and C, for two different measurement heights. Figure 3 considers measurements at 50 m altitude. This altitude corresponds to the lowest scan angle in elevation plane (the beam pointing direction is 0 degrees, resulting when the tilted antenna is steered to -6 deg with respect to the antenna broadside). Figure 4 shows the resolution at 3 km of altitude, corresponds to the maximum scan angle in elevation plane of 12 degrees (or a +6 deg electronic scan for the tilted antenna). Worst case resolution is 2 km, 1.4 km, and 1.1 km for configurations A, B, and C, respectively. This factor of ~ 2 variation in spatial resolution for the different configurations results from the degree to which the antenna beam broadens with increasing scan angle.

Whereas the variation in worst case resolution is substantial, the variation in median resolution is substantially less, ranging from .84 km, to .8 km, to .74 km across the three different configurations. This exercise illustrates how larger numbers of sectors (eg, configuration C) result on less degradation in spatial resolution compared with smaller numbers of sectors in the array configuration (configuration A). The exercise also reveals the importance of considering the statistics of the problem, since the variations for worst case are so much larger than those for the median values. The median values are more representative of the overall situation than the worst case values.

The spatial resolution at 30 km in the broadside direction is 0.96 km. This value is 20%, 12%, and 6% less than the median values for configurations A, B, and C, respectively. The variation with height is relatively small as shown by the numbers between Figure 3 and Figure 4 differing by only 11%. A take-away point from this exercise is that, while larger numbers of sectors are better than smaller numbers of sectors, this is not a particularly strong overall driving consideration with we consider the impact of number-of-sectors versus achieved median resolution.

B. Minimum Radar Sensitivity performance model (Z_{min})

The minimum radar sensitivity $Z_{min}(mm^6m^3)$ can be expressed by equation (2) [5].

$$Z_{min} = \frac{CP_{min}R^2\lambda^2L}{P_tG^2\tau\theta_3\phi_3|K_w|^2}SNR \quad (2)$$

where C is a numerical constant with the value 2.5×10^{16} . We compute the sensitivity as a function of spatial geometric and topology for cases A, B, and C with respect to the set of radar specifications given in Table I. In this analysis G is the total gain of the electronic array antenna and it can be calculated considering the antenna gain scan loss using equation (3) below [6] corresponding to a broadside gain of 39 dB

$$G(\theta, \phi) = \frac{4\pi d_x d_y N_x N_y}{\lambda^2} [1 - |\Gamma(\theta, \phi)|^2] \cos(\theta) \quad (3)$$

where, d_x and d_y represent the unit cell dimensions of the antenna elements on the array, N is the total number of elements in the array in the x (azimuth) and y (elevation) dimensions previously discussed. Γ represents the active reflection coefficient of the active element which changes as a function of the beam position. The gain scan-loss is represented by $(1 - |\Gamma(\theta, \phi)|^2) \cos(\theta)$ and can be approximated $\cos(\theta)^{1.2}$ for practical considerations [4]. SNR represents the signal-to-noise ratio required and for this analysis 0 dB is considered. P_t is the radar transmit power in kW. For this analysis pulse compression is assumed as shown in Table I such that the peak power of the antenna panels is in the 100 W region. Figure 5 shows the worst case sensitivity for the three sector-configurations for measurement height of 50 m. Figure 6 shows the case for 3.18 km measurement height. It should be pointed out that at lower scanning angles

(less than 12 degrees), three zones, or rings sections with different sensitivity are shown in these plots. These zones correspond to the use of a series of three increasing pulse-widths to both increase sensitivity and minimize eclipsing (not being able to receive and transmit at the same time) in the chirp waveform design. Figure 5 and Figure 6 illustrate how

TABLE I
RADAR SYSTEM PARAMETERS

Parameter	Symb	Units	Value
Frequency	f	GHz	9.6
Peak transmitter power	Pt	W	100
E-Plane beamwidth (broadside)	θ_3	deg	1.8
H-Plane beamwidth (broadside)	ϕ_3	deg	1.8
E-Plane scan range (broadside)	$\Delta\theta$	deg	12
H-Plane scan range(broadside)	$\Delta\phi$	deg	60-90-120
Signal to Noise Ratio	SNR	dB	0
Noise figure	NF	dB	4.5
Gain (at broadside)	G	dB	39
Maximum radar range	R	km	31
Range resolution	ΔR	m	25
Bandwidth	BW	MHz	6
Pulse repetition frequency	PRF	Hz	3399
System loss (l)	L	dB	2
Pulse width	τ	μs	4.16-41.67
Pulse compression gain	PCG	dB	14-24
Minimum detectable signal	$P(min)$	dBm	-103.6

the broadening beamwidth effect and gain-scan loss impact minimum radar sensitivity for a single radar node. Compared with the broadside case the worst-case sensitivity degradation is 4, 2 and 0.8 dB for configurations A, B, and C respectively. Corresponding median degradation values are smaller, at 1.1, 0.6 and 0.3 dB.

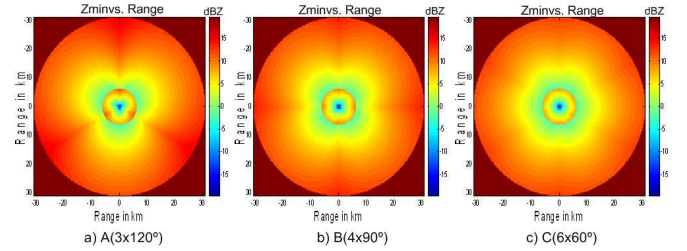


Fig. 5. Z_{min} (worst): a) 15.7 dBZ, b) 13.6 dBZ and c) 12.4 dBZ. Z_{min} (median): a) 9.71 dBZ, b) 9.21 dBZ and c) 8.85 dBZ. θ_o : +6 deg and H:50 m

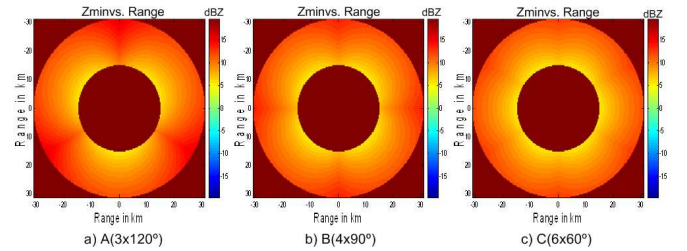


Fig. 6. Z_{min} (worst): a) 15.8 dBZ, b) 13.6 dBZ and c) 12.4 dBZ. Z_{min} (median: a) 10.6 dBZ, b) 10.2 dBZ and c) 9.81 dBZ. θ_o : +6 deg and H:3.18 Km

C. Dual polarimetric performance model

Polarimetric observations are increasingly being considered in weather radar systems [7]. In the US, the NEXRAD system is being outfitted with dual-polarization upgrades, for example. Moreover, at the X-band wavelengths associated with dense radar network designs, the use of polarimetric observations is strongly indicated as one of the primary means to compensating for attenuation. In this section we address the errors associated with imperfect polarization performance in the electronically scanned antenna design. Well matched co-polar beam patterns at vertical and horizontal polarizations, low cross-polarization levels, and high polarization purity are desired in polarimetric weather radars. Two key measurements obtained from polarimetric weather radars are the differential reflectivity (Z_{dr}) and the linear depolarization ratio (LDR). An approach to assessing the polarization performance of a polarimetric design is to simulate the measurement that would be obtained for a uniformly filled volume with identically spherical scatters, given the theoretical (or experimentally obtained) power measurement patterns of the actual antenna, since in this case any measured values of Z_{dr} and LDR that deviate from ideal would be indicative of the error caused by the antenna only [7]. For such a simulation, Z_{dr} represents the differential reflectivity bias error (Z_{dr}^b) and LDR is called integrated cross-polarization ratio ($ICPR$) [8]. The expression of the Z_{dr}^b is defined in equation (4) taken from [7].

$$Z_{dr}^b = \frac{\int |f_{hh}^2 + f_{hv}^2|^2 d\Omega}{\int |f_{vh}^2 + f_{vv}^2|^2 d\Omega} \quad (4)$$

where f_{hh}, f_{hv}, f_{vv} and f_{vh} represent the magnitude of the power patterns of a linear polarized antenna, where the first sub-index represent the polarization in transmit mode (h : horizontal and v : vertical) and the second sub-index represent the polarization in the reception mode. The $ICPR$ is expressed in equation (5) taken from [7].

$$ICPR = \frac{\int f_{hh} f_{hv} d\Omega}{\int f_{hh}^2 d\Omega} \quad (5)$$

To assess the polarization performance for the antennas being considered here, simulated patterns for f_{hh}, f_{hv}, f_{vv} and f_{vh} were performed for tilted planar arrays using the finite array tool of HFSS for sector configurations A, B, and C. To simplify the design simulation process a uniform amplitude distribution was considered. The aperture coupled patch antenna was selected as a radiating element because it offers multiple advantages over the direct contact counterparts. Principally, it minimizes the effect of surface waves and spurious radiation of the feed which improves the element pattern symmetry and polarization purity. Table II shows worst case scenario results of the Z_{dr}^b and ($ICPR$) for the three different sector-configurations (A, B and C) for broadside and the maximum scan beam positions in azimuth (60, 45 and 30 deg) and elevation plane from 0 to 12 degrees (6 deg). Poor performance is indicated in configuration A. This

effect can be attributed to the lattice array configuration, mutual coupling, and polarization changes as a function of the scanning beam. A variation around 22 dB in the $ICPR$ is produced in configuration A with respect to the best values obtained at broadside, 15 dB and 9 dB represent the variation of configurations B and C with respect to best values obtained at broadside. Similarly with Z_{dr}^b , large errors are observed for a wide scan range in the azimuth plane. These errors can be attributed to the large mismatch of the beam pattern produced by the large broadening beamwidth effect and the scan losses (case A and B). The last column in Table II shows the interpolated values of the induced error in Z_{dr}^b (*) as a function of the cross-polarization ration calculated by Wang at [9]. This calculation was performed for light rain assuming matched beam patterns calculated for alternated mode configuration. Although there are large errors in Z_{dr}^b due to the mismatch beam patterns, these are known and can be compensated during the calibration process. Nevertheless the error in the Z_{dr}^b produced by the cross-polarization represent an important limitation for steering antennas that require scan ranges larger than 30 deg.

TABLE II
SCANNING PERFORMANCE IN FUNCTION OF POLARIZATION AND MISMATCH BEAM PATTERNS

Config	Azimuth (deg)	$ICPR$ (dB)	Z_{dr}^b (dB)	Z_{dr}^b (*) (dB)
A(3x120)	± 60	-6	6.6	~ 1.0
B(4x90)	± 45	-13	3.4	~ 0.8
C(6x60)	± 30	-19	1.3	~ 0.2

Z_{dr}^b (*) calculated for light rain and matched co-polar beams [9].

III. PERFORMANCE MODEL FOR A DENSE RADAR ENVIRONMENT

We now consider the performance of networked radar designs for configurations A, B, and C. A separation of 30 km between nodes was considered for all configurations as shown in the profile-view geometry of three overlapping radar nodes in Figure 7.

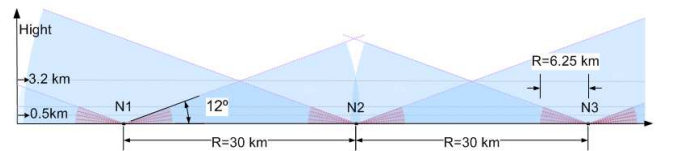


Fig. 7. Elevation cut of overlapping coverage of three radars in network

A. Azimuth resolution performance model (A_{zr})

Figure 8 and Figure 9 show the top view of the azimuth resolution at 50 m and 3.2 km altitude. In both cases the sector-configuration C composed by 6 sectors of 120 degrees

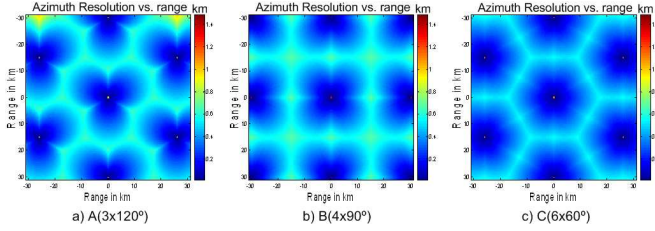


Fig. 8. A_{zr} (worst): a) 0.97 km, b) 1.4 km and c) 1.1 km A_{zr} (median): a) 0.41 km, b) 0.42 km and c) 0.36 km. θ_o : -6 deg, and H:50 m

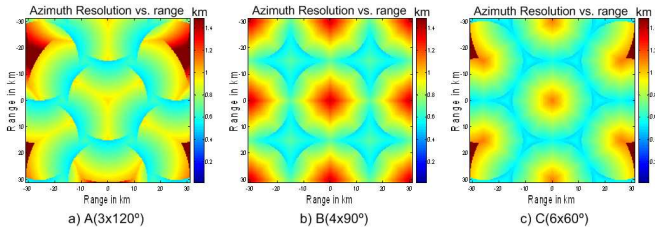


Fig. 9. A_{zr} (worst): a) 1.9 km, b) 1.4 km and c) 1.1 km A_{zr} (median): a) 0.79 km, b) 0.79 km and c) 0.72 km. θ_o : $+6$ deg, and H:3.18 Km

each, gives the best azimuth resolution. Configuration C improves the azimuth resolution (median values) in about 11% with respect to the others (B and A) in both altitudes (5 m and 3.2 km). In comparison with a single node around 100% represents the improvement in azimuth resolution for all three configurations for the same area. Additionally, 100% of the total volume required is covered with a median azimuth resolution of 0.8 km.

B. Minimum radar sensitivity (Z_{min})

Figure 10 and Figure 11 show the minimum radar sensitivity in a networked configurations A, B, and C. Configuration C shows the best performance, about 1 to 3 dB better than configurations A and B.

IV. SYSTEM COMPLEXITY CONSIDERATIONS

In this section we consider aspects of the technological complexity and cost issues associated with low-power networked phased arrays. Two important parameters in the design of such panels are the panel peak power level and the total number of active radiating elements needed to fabricate each panel. Today's high-power multi-function phased array radars cost on the order of \$1 M per square meter of antenna aperture. The T/R modules in these antennas typically transmit up to 10 Watts each and cost on the order of \$1 k per module. The technology envisioned here is entirely new and has not yet been fabricated to the point of fielding low-cost phase-phase electronically steered array radars for meteorological sensing. High-volume-produced radars have been successfully developed and brought to market for collision avoidance in automobiles, and there is experience for costing semiconductor based projects based on experience from the

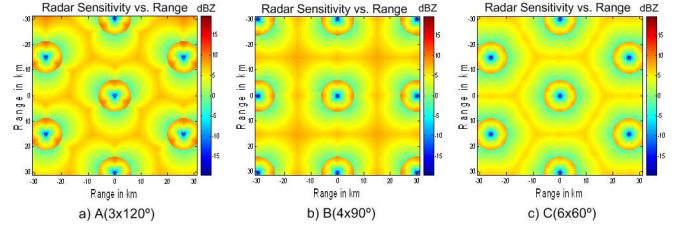


Fig. 10. Z_{min} (worst): a) 11.5 dBZ, b) 13.4 dBZ and c) 12.1 dBZ, Z_{min} (median): a) 4.54 dBZ, b) 4.52 dBZ and c) 3.7 dBZ. $P_t=100$ W/sector, θ_o : -6 deg

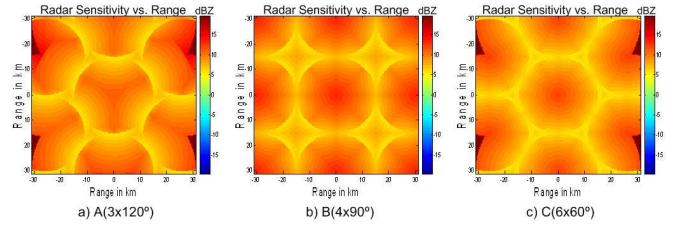


Fig. 11. Z_{min} (worst): a) 15.3 dBZ, b) 13.5 dBZ and c) 12.3 dBZ, Z_{min} (median): a) 9.26 dBZ, b) 9.06 dBZ and c) 8.56 dBZ. $P_t=100$ W/sector, θ_o : $+6$ deg

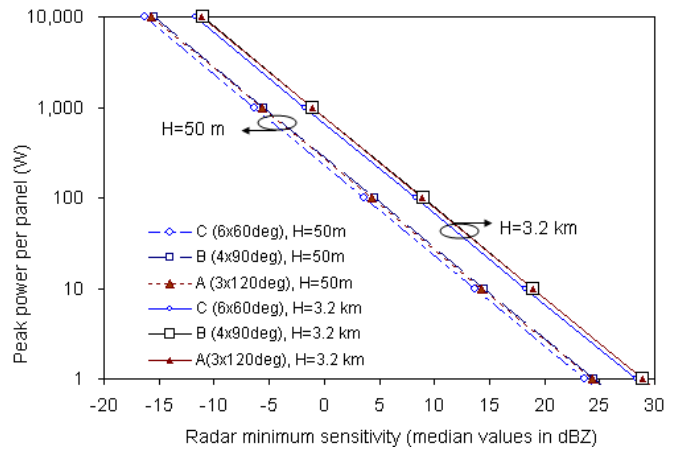


Fig. 12. Z_e (median) versus peak power per sector for A, B and C in a network environment.

wireless sector and the published semiconductor roadmap, and these provide some basis for developing rough, order-of-magnitude, estimates of the costs of the panels discussed here. The total number of radiating elements, and associated transmitter/receiver (T/R) channels per panel are 2,944; 2,760; and 2,482 for configurations A, B, and C, respectively. The corresponding total number of elements per node (# elements x # panels) are 8,832; 11,040; and 14,904 as summarized in Table III. Whereas modern defense-related phased arrays are high performance, high-power systems, the arrays considered here are low-power systems instead. Figure 12 plots the peak power required per panel as a function of desired sensitivity level in Z_{min} for networked radar configurations A, B, and C at both 50 m and 3.2 km measurement heights. The curves show that a sensitivity level of 10 dBZ (which represents the reflectivity associated with a clear-air "bright line" resulting from insect scattering) can be achieved using panel power

levels ranging from a few 10's of watts to 90 W, depending on configuration [11]. Taking the upper limit of this range, and assuming the antenna is illuminated with an amplitude distribution of -25 dB Taylor in order to reduce the sidelobe level in the antenna pattern, the approximate power level required per T/R module are: 107, 114 and 118 mW for configurations A, B and C respectively. At these power levels the current technologies available for X-band are: GaAs 0.15 μm , SiGe 0.5 μm , and RF-CMOS 0.18 μm . The current cost for a GaAs 0.15 μm die of 1 mm^2 is 6 times the cost of SiGe 0.5 μm and 5 times RF-CMOS 0.18 μm . Of these, SiGe 0.5 μm appears to be the lowest cost option based on semiconductor substrate costs alone. The last three lines of Table III give very rough estimates of the costs of panels based on substrate costs, assuming the T/R channel functions can be achieved using 15 mm^2 of area each and (roughly) assuming a \$2.2 estimated cost for each die [12]. Further, assuming that the cost of the radiating element, RF material and fabrication, result in a total per-element cost of \$3.2 dollars, the per-panel costs are \$6.5 k, \$8.1 k, and \$5.7 k for configurations A, B, and C. When multiplied by the number of panels per node (eg, 3, 4, or 6 for Configurations A, B, and C), we estimate that the cost per radar ranges between \$30 k and \$50 k as summarized in Table III.

TABLE III
PERFORMANCE COST MODEL

Parameter	units	A(3x120)	B(4x90)	C(6x60)
Unit cell size	cm	1.6x2.2	1.7x2.2	1.9x2.2
No. elements	-	64x46	60x46	54x46
No. elements	-	2944	2760	2484
A_{zr} (worst)	km	1.90	1.40	1.10
A_{zr} (median)	km	0.79	0.78	0.72
Z_{min} (worst)	dBZ	15.30	13.5	12.3
Z_{min} (median)	dBZ	9.26	9.06	8.56
Z_{dr}^b	dB	6.60	3.40	1.30
Z_{dr}^b (*)	dB	~1.0	~-0.8	~-0.2
ICPR	dB	-6.0	-13.0	-19.0
Active element cost	\$	3.11	3.17	3.29
Antenna cost per sector	\$	6,565	8,127	5,788
Antenna cost per node	\$	27,482	34,992	48,967

V. REFERENCES

- [1] NRC (National Research Council), "Weather Technology Beyond NEXRAD", *National Academy Press, 2002, Washington DC.*
- [2] D.J. McLaughlin et al., "Distributed Collaborative Adaptive Sensing (DCAS) for Improved Detection, Understanding, and Predicting of Atmospheric Hazards", in *Proc. of 85th AMS Annual Meeting, 2005, San Diego, CA.*
- [3] Gerald V. Trunk., "Optimal Number of Phased Array Faces for Horizon and Volume Surveillance- Revisited", in *IEEE, 2003.*
- [4] R. J Mailloux., "Phased Array Antenna Handbook", in *Artech House, 2005, Norwood, MA, USA.*
- [5] R. J. Doviak, and D.S Zrnic., "Doppler Radar and Weather Observations.", in *Academic Press, 2nd. edition, New York, USA.*
- [6] D. M. Pozar., "The Active Element Pattern", in *IEEE Trans. Antennas and Propagation.,42,8,1176-1178.*

- [7] D.A. Brunkow et al., "A Description of the CS-CHILL National Radar Facility", in *J. Atmos. Oceanic Technol.,17,1596-1608.*
- [8] V. Chandrasekar and R. Jeffrey Keeler., "Antenna Pattern Analysis and Measurement for Multiparameter Radars", in *J. Atmos. Sci.,10,674-683.*
- [9] Y. Wang, V. Chandrasekar and D.J. McLaughlin., "Antenna System Requirement for Dual Polarized Radar Design in Hybrid Mode of Operation", in *Merereology, Alburque, NM.*
- [10] Samuel P. Williamson et al., "Federal Research and Development Needs and Priorities of Phased Array Radar", in *June 2006.*
- [11] D.J. McLaughlin et al., "Distributed Weather Radar Using X-Band Active Arrays", in *IEEE Radar 2007 Conference, April 2007, Waltham, MA.*
- [12] IC Cost Modeling., "IC Knowledge" in *Georgetown.*